Communications
Research Centre
Centre de recherches
sur les communications

The Effects of Antenna Array Geometry and Element Pattern uncertainty on High-Latitude HF Direction Finding

by

Robert W. Jenkins

CRC REPORT NO. 97-006

December 1997
Ottawa

Industry Canada Industrie Canada

The work was sponsored by the Department of National Defence, Research and Development Branch, under Project No. 998445419.

Canada

ABSTRACT

Simulation studies are described which model the performance of a sampled-aperture HF direction-finding (DF) system operating with specified array geometries in the presence of both single-reflection (point-source) and multiple reflection/scattering (extended-source) ionospheric radio propagation typical of observed high-latitude nighttime conditions. A multiple-direction estimator was used to obtain direction estimates; the deterministic maximum-likelihood algorithm was selected for this, following a comparison between it and the MUSIC algorithm. Array pattern errors, based on previous phase and amplitude pattern measurements and numerical modelling, were included in the simulation. The performance is characterised in terms of the ability of the DF system to see a weaker point source in the presence of the extended source. The array apertures in wavelengths (or alternatively operating frequencies for a fixed-size array) over which good performance was obtained was limited at the low end by the resolving power of the array, and at the high end by the narrow array beamwidth and the limited number of directions available to the DF algorithm to describe the situation. Pattern errors reduced performance significantly; much more at small array apertures (2.5 wavelengths or less) than at larger apertures (5 wavelengths or more). Of the four 12-element array geometries tested, the 'star' array, consisting of three arms with its smallest spacings at its extremities, performed best over the widest range of aperture sizes (or alternatively, operating frequencies).

RÉSUMÉ

On décrit des études par simulations qui établissent un modèle du rendement d'un système goniométrique (DF) haute fréquence (HF) par échantillonage d'ouverture pour quelques dispositions spécifiques du réseau d'antennes en présence simultanée d'un signal principal provenant d'une réflection ionosphérique simple et d'un signal multiple de réflection/diffusion (source étendue) ionosphérique typiques de la propagation radio en haute latitude durant la nuit. Un estimateur de direction multiple fut utilisé pour établir une évaluation des directions d'incidence; l'algorithme déterministique la probabilité maximale fut utilisé à cet effet à la suite d'une comparaison de celui-ci avec l'algorithme MUSIC. Les erreurs du diagramme du réseau d'antennes, sur la base combinée de mesures préalables de phase et d'amplitude du diagramme de rayonnement et de l'évaluation numérique par modèle, furent incluses dans la simulation. Le rendement du système DF est évalué à sa capacite de récupérer un signal faible en présence d'un signal parasite étendu sur une grande plage angulaire. L'ouverture du réseau exprimée en longueurs d'onde (ou altermativement en fréquences d'opération pour un réseau de dimensions fixes) pour laquelle le rendement est jugé satifaisant est limité au bas de son échelle par le pouvoir de résolution du réseau et au haut de son échelle par l'étroitesse du faisceau et le nombre limité de directions disponibles à l'algorithme DF pour décrire la situation. Les erreurs dans le diagramme de rayonnement réduisent considérablement le rendement du système, beaucoup plus aux faibles ouvertures du réseau (2.5 longueurs d'onde ou moins) qu'aux grandes ouvertures (5 longueurs d'onde ou plus). Des quatre dispositions géométriques des réseaux à 12 éléments étudiées, le réseau en 'étoile' formé de trois branches avec espacement minimum aux extrémités a donné un rendement maximum pour la plus grande étendue de grandeurs d'ouverture (ou d'une façon équivalente de bande de fréquences d'exploitation).

EXECUTIVE SUMMARY

In developing HF direction-finding systems for use at high latitudes, it is important to consider the unique radio propagation environment present at those latitudes, and use array geometries and DF algorithms appropriate for that environment.

The propagation environment is particularly difficult under nighttime conditions, where the ionosphere which makes propagation possible beyond the horizon is characterized by low electron densities and irregular moving patches or blobs that may scatter or reflect radio waves from many points. The result is a radio signal having many directions whose bearings are different from that of the transmitter. At the same time, sporadic-E ionization may also be present which yields a single weaker signal direction with a bearing close to that of the transmitter. A system requirement for successful DF operation at these times is the ability to see and identify a single signal direction, in the presence of a spread set of directions whose composite signal strength is greater.

This requirement implies that a multiple-direction estimation technique is required for the DF algorithm. Current techniques include the widely used MUSIC algorithm, and the more computation-intensive maximum-likelihood algorithm. Both algorithms require that the number of signal directions be assumed, and set to a value less than the number of antennas.

The limited number of directions means that a spread set of directions consistent with moving patches may not be accurately described, since there are many more directions present than can be estimated by the algorithm. However, if the array aperture is not too large, the array beamwidth will be wide enough that the spread set can be 'covered' by a number of beams, less than the number of directions available, leaving a direction free to attach to a weaker single-direction sporadic-E signal.

These algorithms require knowledge of the radiation patterns, both gain and phase, of the element antennas in the DF array. This knowledge can come through making educated simple assumptions. (In the case of an array of vertical whip antennas, pattern assumptions often made are an azimuth-independent gain and phase responses consistent with a plane-wave signal propagation from the direction of interest.) Pattern knowledge can also come from numerical modelling, or actual measurements, which are progressively more accurate than assumptions.

Uncertainties in the element patterns affect the accuracy and sensitivity of DF algorithms, especially in seeing and estimating the directions of weaker signals. Reducing these uncertainties may be critical to the success of a DF system operating in high-latitude nighttime conditions. From previous measurements and modelling studies of the element patterns of the 'Vortex' array in the Ottawa area, the uncertainties inherent in the three techniques: simple assumption, modelling, and measurement, were estimated.

This paper presents the results of a simulation study to assess the effects of array geometry and element pattern uncertainty on DF systems operating in high-latitude nighttime conditions.

The signal environment consisted of a spread set of directions (spread source) covering 25° in azimuth, and a single weaker direction (point source), removed in azimuth from the spread source by various amounts. The performance criterion used was that of point-source visibility: how much weaker in power can the point source be, relative to the spread source, and still be seen.

Four different 12-element array geometries of vertical whip antennas were simulated, each having a similar range of apertures (as measured in wavelengths, which is equivalent to a range of operating frequencies for a fixed physical size). These included the Vortex array, a log-spiral array, a centered-circle array, and a three-prong 'star' array. Two levels of pattern uncertainties were modelled: large, consistent with those errors found for simple assumption or modelling, and small, consistent with measurement errors.

The direction estimation techniques included MUSIC and deterministic maximum likelihood. The AIC criterion, based on a technique which examines the eigenvalues of the covariance matrix, was used to set the number of directions present. Initial studies showed the maximum-likelihood technique to perform better than MUSIC, owing mainly to the tendency for MUSIC to estimate false signal directions. For this reason, and also since maximum likelihood was based on an optimal approach, the maximum-likelihood technique was used for the remainder of the study.

The simulations clearly demonstrated that array aperture and geometry are critical factors in the ability of a DF array to see weak signal directions in the presence of stronger spread signals. The useful array aperture is limited, on the low end, by the resultant low resolving power of the array, and on the high end by the resulting narrow array beamwidth and the greater number of directions required to describe the spread source before any directions can be allocated to the point source. The range of useful apertures varies with array geometry. Of the array geometries tested, the star array performed best, having the largest range of useful apertures (or for a fixed size, the largest useful frequency range), from 3 to 7 wavelengths, as well as having the best performance over its useful range (point source visible down to 24 dB below the spread source, at a bearing separation of 15°, in the absence of pattern errors). The star array was the only array of those tested to have its closest spacings at its extremities, resulting in the largest proportion of large interelement spacings.

The influence of pattern uncertainties on performance was quantitatively demonstrated in the simulations. Point-source visibility was adversely affected by pattern uncertainties, substantially for small array apertures and less (but still noticeably) for larger apertures. The results illustrate the need to reduce the pattern uncertainty in operational arrays intended for high latitudes.

Another study planned for the near future is an examination of existing high-latitude nighttime sampled-aperture and oblique ionosonde data to determine the incidence of occurence of sporadic-E signal propagation. A modified DF algorithm, developed at DREO, is currently undergoing evaluation. This algorithm is based upon the stochastic maximum-likelihood technique, and, instead of using a limited number of single directions to match the observed signal environment, it assumes a number of spread sets of directions, the ranges of which are varied to fit the observations.

TABLE OF CONTENTS

LIST OF ILLUSTRATIONS

1.0 INTRODUCTION

High-latitude HF direction-finding (DF) during darkness is often characterised by signals arriving from a changing range of directions as a result of reflection or scattering from moving ionospheric F-region features such as 'blobs' or 'patches' convecting across the polar cap [1, 2]. These directions tend to cover the solid angles subtended by the moving features, and thus are not an accurate indicator of transmitter direction. In order to properly assess the situation, a multiple-direction estimation technique such as MUSIC or maximum likelihood is required. At these same times, the occasional appearance of sporadic E-layer ionization may give rise to signal propagation in the great-circle direction at lower angles consistent with E-layer reflection [2]. The sporadic-E signal may be weaker than the higher-angle direction-spread F-region signals due to the poor low-angle gain of HF antennas. A multiple-direction estimation algorithm is needed to see the sporadic-E signal direction and thus obtain a reliable direction estimate at these times [3].

Current multiple-direction estimation algorithms such as MUSIC or maximum likelihood require an estimate of the number of directions present, usually limited to a value below that of the number of elements in the antenna array. The high-latitude nighttime situation involving moving patches represents many more signal directions than can be handled by these algorithms. When applied to this situation, these algorithms apply their limited number of directions to describe the observed signal environment as closely as they can; this results in direction values scattered over the solid angle subtended by the patch. Random changes in these individual estimated directions typically occur within periods of a second or so [3]. When a weaker sporadic-E signal is also present, these algorithms will see it as well, provided that the patch does not use up all the direction estimates available to the algorithm. An array aperture that is too large will result in a beamwidth that is so narrow that the available number of direction estimates will be used up in attempting to cover the solid angle of the patch, leaving none for the weaker sporadic-E signal. A smaller aperture causes the array to have a sufficiently large beam that the patch may be covered by fewer than the available directions, permitting the sporadic-E signal to be described by a remaining direction. If the aperture is too small, however, the sporadic-E signal may not be distinguished from the stronger patch signal because of the low resolving power of the array. The aperture and, by inference, the array geometry are important to the performance of multiple-direction estimating DF systems in the high-latitude nighttime signal environment.

Another important element in the application of sampled-aperture antenna arrays in HF direction-finding (DF) is the knowledge of the actual element radiation patterns. Knowledge of both phase and amplitude patterns is needed to implement the higher-performance multi-direction DF algorithms, such as MUSIC and maximum likelihood, coming into use with the advent of increased processing capability [4]. Thus the effect of pattern estimate uncertainties becomes an important consideration. These uncertainties can be expected to affect not only the accuracy of the ensuing direction estimate, but also the dynamic range of the process, i.e., the range of powers over which signal directions can be estimated. In addition, they are likely to have a far greater effect on the direction estimates for weaker signals in the presence of strong signals, since the errors related to the stronger signals will cause significant perturbation in estimating the contributions of the weaker signals.

1.1 THE POLAR RADIO PROPAGATION ENVIRONMENT AND ITS INFLUENCE ON HF DIRECTION FINDING

It is worthwhile reviewing the high-latitude HF radio propagation environment in greater detail, prior to considering appropriate DF systems for use in that environment. This environment is dominated by the ionosphere on which it depends.

The polar ionosphere is a highly variable, often turbulent medium [1, 2], owing to its locations near the magnetic poles of the earth and its consequent connection via the earth's magnetic field lines to the solar wind, a charged plasma consisting of protons, electrons, and associated magnetic field lines that moves outward from the sun past the earth. The moving solar wind sets up a two-cell convection pattern in the ionosphere over the polar regions [8], with an antisunward motion at the highest latitudes (polar cap), and a returning sunward motion at lower (auroral and sub-auroral) latitudes. Solar activity causes changes in the solar wind, which in turn affects the convection and other features of the high-latitude ionosphere.

Under sunlight conditions, the polar ionosphere is reasonably well-behaved. The photoelectric process provides a steady source of ionospheric electrons, and the relatively high conductivity that occurs in the E region of the ionosphere causes any localized ionospheric enhancements to decay rapidly. The same is not true under darkness conditions. The E layer is normally not present and ionospheric enhancements decay much more slowly. The lack of photoelectric production allows the ionosphere to gradually deplete to levels of low electron density, through the motion of electrons and positive ions upward along the magnetic field lines. Large-scale enhancements drift backward from the sunward side where they are created[1,9] to the antisunward side of the earth. The gradient drift instability [1] gives rise to small-scale ionospheric irregularities to be produced as these features move. At the same time, precipitating particles in the polar regions [10, 11] can cause additional enhancements. Sporadic E-layer ionization, which may be related to particle deposition as well as other time-varying ionospheric features, is sometimes present.

The ramifications for HF radio propagation are substantial. An irregular ionospheric enhancement will reflect radio waves from many places over its surface, causing a radio signal to arrive at a receiving site from many directions within the solid angle spanned by the feature at the receiver. In addition, radio waves may be scattered from small-scale irregularities, so that they also arrive at the receiving site from many directions, also covering the solid angle spanned by these irregularities. Thus, a direction-finding system will see many signal directions not necessarily close to the direction of the signal transmitter, rather than the single great-circle direction that occurs with a well-behaved horizontally stratified ionosphere. As the ionosphere in the polar cap is moving across the polar cap in the antisunward direction, these features and their related signal directions will also be seen to move.

In a set of interferometer measurements conducted at Alert, N.W.T. in November, 1990, a large number of off-great-circle directions were noted for transmissions from Thule, Greenland [12]. For a substantial portion of the time, the directions were seen to be scattered from one measurement to the next, over 20° or more in azimuth. Also the cluster of directions was observed to

move with time, sometimes over more than 90° in azimuth, over tens of minutes. The observed positions and motions were consistent with an antisunward convective flow of F-region ionospheric enhancements. Separate modelling studies [3], invoking the different mechanisms of scattering from field-aligned irregularities and multiple reflections from irregular surfaces, were able to reproduce many of the observed features.

Another feature seen in the interferometer data from Thule was the occasional appearance of a short-lived (several minutes) consistent set of directions close to great-circle, with elevation angles consistent with an E-layer reflection. This phenomenon, which occurred in the midst of the moving spread directions, was interpreted as being due to sporadic-E reflections. The direction-finding estimate, at these times, gave the true transmitter direction, rather than the enhancement direction as was otherwise the case. As the interferometer technique has the property of selecting the direction with the strongest signal, the great-circle signals could only be seen when the sporadic-E signal was the strongest. which in the case of the November 1990 measurements was only one percent of the time.

It is desirable to increase the visibility of sporadic-E signals, in order to obtain accurate direction estimates which would otherwise not be available. A multi-direction algorithm such as MUSIC can be expected to see the sporadic-E signals more often than a single-direction estimator. An appropriate criterion with which to evaluate the success of such techniques is how far below the other signals the sporadic- E signal can be in power and still be seen. A simulation study [3] using several array geometries, and a path and frequency similar to the Thule measurements, estimated that sporadic-E signals could be as much as 21 dB below the other 'spread' signals and still be seen using MUSIC. Antenna-array gain errors were not included in this study. As array pattern errors have a strong influence on performance, especially for weak signals in the presence of strong signals, it is important to extend this study to include such errors.

1.2 AIM OF THE REPORT

This report describes a study of the effect of array geometry and element-pattern uncertainties on the performance of potential HF direction-finding systems operating at high latitudes during darkness hours. The modelled environment includes both a set of 'spread' signal directions (referred to herein as an extended source), uniformly distributed over a specified range of azimuths and elevations, and a weaker single signal direction (referred to herein as a point source), at a specific azimuth and elevation. Various directions and azimuthal separations between point source and extended source are simulated. Several levels of antenna-pattern uncertainty are simulated, consistent with the approaches to pattern estimation described in the next section. Two direction-finding techniques are tested: MUSIC and deterministic maximum likelihood. Various antenna array geometries and operating frequencies are used. The goal is to find the best configurations, i.e., adaptive algorithm and array geometry for use in the modelled nighttime high-latitude environment, and to estimate the performance attainable by such configurations, for the levels of antenna pattern uncertainty likely to be incurred.

2.0 RADIATION PATTERN UNCERTAINTIES

The element antenna radiation patterns may be obtained through three basic approaches. The first, and simplest, approach often applied to arrays of simple elements is to assume the amplitude (gain) pattern given by theory for individual elements, and a position-dependent phase response consistent with plane-wave propagation, for each element. The second approach is to perform numerical modelling, taking into account interactions between all radiating elements in the array and its vicinity, and a simplified ground such as a uniform flat ground. The third approach involves actual measurement of the patterns. Recent pattern measurements and modelling [5,6,7] on a representative antenna array have provided estimates of the pattern uncertainties inherent in each approach.

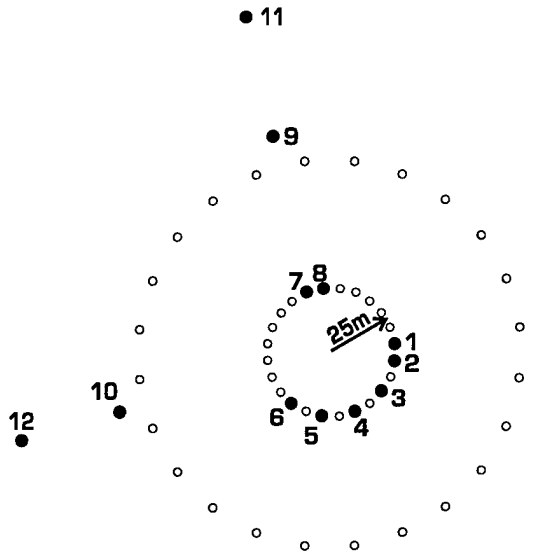

Figure 1. Plan geometry of Vortex antenna array. Numbered elements are used in the sampled-aperture array.

The pattern measurements [5] and numerical modelling [6] conducted on an HF array in the Ottawa area provided an estimate of the typical uncertainties that could be expected in assuming antenna pattern gains and phase responses for a sampled-aperture direction-finding system. The array in question consisted of eight elements from the inner circle of a Pusher array, plus four additional elements placed along two axes at right angles, as shown in Figure 1. This array, referred to herein as the 'Vortex array', is similar to one used in recent high-latitude HF DF measurements. The selected elements are 20 ft. vertical whip antennas, as are the remainder of the inner-circle Pusher elements. The outer-circle Pusher elements are 40 ft. whip antennas.

The first and simplest approach for obtaining patterns for this antenna array is to assume the azimuth-independent gains expected of isolated vertical whip antennas, and the relative phase responses given by the antenna locations and a plane-wave calculation for the direction of interest. Based on the measurements, the errors inherent in this approach were estimated. The errors inherent in the measurements and modelling approaches were also estimated [6, 7].

The estimated errors are given in Tables 1 and 2 for several operating frequencies, several representative antennas of the Vortex array and at an elevation angle of 11°. (The errors were found to be almost independent of elevation angle below 20° elevation.) The errors found for the measurement technique were substantially less than for the modelling and simple-assumption techniques, which were roughly similar. While there are some variations between antennas in the modelling and simple-assumption errors, a general trend can be derived from these values. The tendency is for the gain errors to be almost frequency-independent, and the phase errors to vary only slightly less than proportionally with frequency.

Table 1: RMS gain errors averaged over azimuth, found for several representative elements of the Vortex array, at an elevation angle of 11°

	ε_{meas} (dB)			ε_{mod} (dB)			ε_{assmp} (dB)		
MHz	ant#5	ant#9	ant#11	ant#5	ant#9	ant#11	ant#5	ant#9	ant#11
5.1	0.23	0.24	0.27	1.04	0.66	0.75	0.86	0.69	0.71
11.5	0.70	0.69	0.72	0.52	1.33	0.75	0.89	1.46	0.39
18.0	0.37	0.32	0.35	0.64	0.77	0.86	0.63	1.51	0.70

Table 2: RMS phase errors averaged over azimuth, found for several representative elements of the Vortex array, at an elevation angle of 11°

	ε_{meas}			ε_{mod}			ε_{assmp}		
MHz	ant#5	ant#9	ant#11	ant#5	ant#9	ant#11	ant#5	ant#9	ant#11
5.1	0.9°	1.1°	1.1°	9.0°	7.8°	7.8°	3.5°	3.6°	3.1°
11.5	1.3°	2.1°	2.8°	6.0°	6.2°	4.4°	6.6°	7.9°	5.4°
18.0	1.6°	2.1°	2.8°	7.1°	6.5°	6.4°	10.7°	8.9°	8.3°

On this basis, two levels of error were obtained for the purposes of the present work: large errors representative of those introduced by using overly simple assumptions such as plane-wave phase response and azimuth-independent gain patterns, or numerical modelling in our case; and small errors typical of what may be obtained from making actual pattern measurements. The average rms values found from the previous studies were interpolated to obtain corresponding representative values for the frequencies used in the present study. These are shown in Table 3.

Table 3: RMS antenna gain and phase response errors simulated for the various frequencies and corresponding antenna apertures used

frequency	aperture	small errors		large errors	
(MHz)	(wavelengths)	gain	phase	gain	phase
2 MHz	1.62 λ	0.19 dB	0.7°	0.58 dB	1.8°
3 MHz	2.43 λ	0.22 dB	1.1°	0.64 dB	2.5°
4 MHz	3.24 λ	0.25 dB	1.3°	0.7 dB	3.0°
5 MHz	4.05 λ	0.27 dB	1.6°	0.74 dB	3.5°
6 MHz	4.86 λ	0.29 dB	2.0°	0.78 dB	4.0°
8 MHz	6.48 λ	0.33 dB	2.5°	0.85 dB	5.0°
10 MHz	8.10 λ	0.37 dB	3.0°	0.93 dB	6.0°

Since actual antenna patterns differ from the assumed ones in a way that varies continuously with azimuth, a functional approach must be used in order to generate 'actual' patterns for the simulation from the assumed patterns and rms errors. The method used was to consider the Fourier (harmonic) components of the azimuthal patterns, and to randomly generate these components according to a mean spectral distribution consistent with that observed. The observations suggested that the mean values of the Fourier components had squared amplitudes decreasing linearly from one cycle over 360° azimuth, down to zero at a cutoff of 15 cycles over 360°; this was the spectral distribution assumed. The actual amplitudes of the Fourier components were then randomly selected according to a Gaussian noise distribution, with the means derived from the rms value, satisfying the requirement that the sum of the mean squared amplitudes was equal to twice the square of the rms error taken from Table 3. The phase of each Fourier component was selected randomly over 2π. The differences between the assumed patterns and the simulated 'actual' patterns were completely specified in terms of the Fourier components, which, once generated, could be used to determine each antenna's gain and phase response in any direction.

3.0 ANTENNA ARRAY GEOMETRIES

The four antenna arrays selected for simulation each consisted of twelve vertically oriented whip antennas, whose azimuthal dependence in gain was assumed to be constant, and whose relative phase dependence for any signal direction was assumed to be consistent with a plane wavefront from that direction.

The array geometries are given in Figure 2. The Vortex array and log-spiral array are based on designs that have been previously implemented in experimental systems. The centered circle and three-prong star array were recommended on the basis of good performance in low signal-to-noise situations [13].

The four arrays were scaled so as to have the same physical aperture. This permitted a more direct comparison of the properties of the various antennas, independent of aperture. This required the two previously implemented arrays, Vortex and log-spiral, to be scaled slightly from their original implementations. The apertures, averaged over all azimuths, are given in wavelengths as a function of frequency in Table 3.

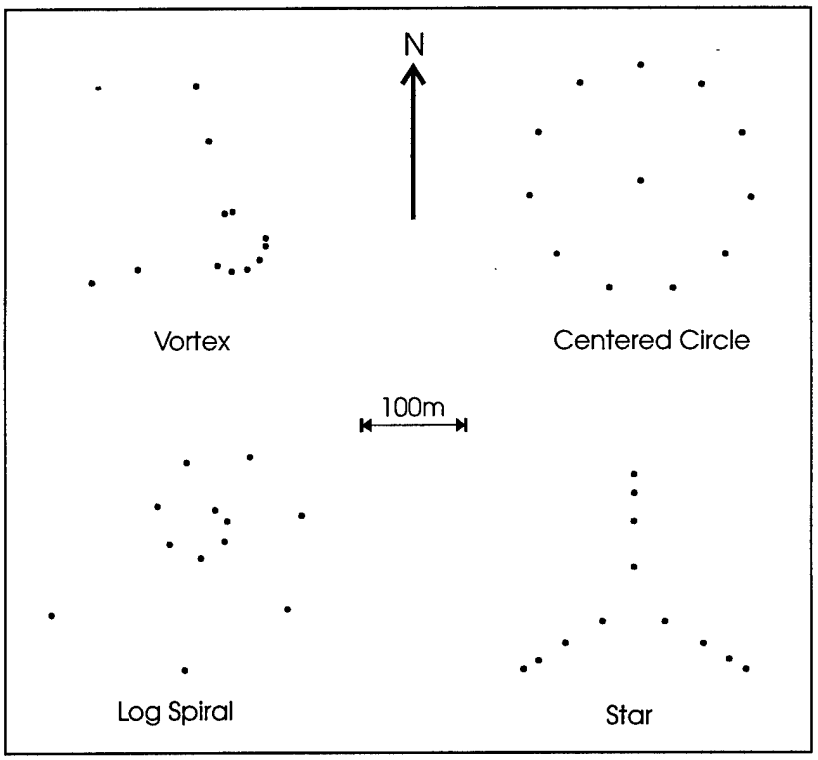

Figure 2. Plan views of simulated antenna arrays.

4.0 DIRECTION-FINDING ALGORITHMS

The direction-finding algorithms used in the simulation were intended for multiple point-source signal direction analysis. These included both the MUSIC [14] and deterministic maximum-likelihood [15] algorithms. The maximum-likelihood approach, while being a more optimal approach for a number of point sources in white Gaussian noise and thus better than MUSIC in low signal-to-noise situations under these conditions [15], requires much more computation.

Both algorithms were attempted in the early stages of the simulation. Based on the findings, the maximum-likelihood approach was found to be best under the simulated conditions, and was selected for more intensive simulation. For both methods, the Akaike criterion [16] with the Lawley approximation [17] (denoted here as the AIC criterion) was used to estimate the number of directions present.

As the simulation included clusters of a large number of signal directions, these techniques could not hope to match the number of directions present, since they were limited to less than the number of array elements. However, as the array beamwidth for any steered direction covered a finite range of directions, it was hoped that these algorithms would be able to approximate the simulated spread set of directions, thereby determining the mean and extent of the spread set, as well as determining the direction of any single-direction signal present.

5.0 SIMULATED SIGNAL ENVIRONMENT

The simulated signal environment was selected to address the high-latitude problem of seeing a relatively weak sporadic-E signal (with a direction close to great-circle) in the presence of stronger signals reflected or scattered from irregular, off-great-circle features.

The signals from a single irregular ionospheric feature were modelled as 1000 signals of equal mean power, from an apparent 'extended source' of distinct directions uniformly distributed in the statistical sense over a portion of the coordinate sphere of 25° azimuthal width, between 10 and 25° elevation. This is typical of the angular spreads observed in signal directions during darkness at high latitudes [12]. The signals from each direction were random with respect to each other in their phase. High-latitude signal propagation in the presence of such features is characterised by Doppler spreading, typically several tens of Hz [18]. This property was simulated by imparting a 20-Hz Doppler spread to each of the 1000 signals separately. This was done by randomly generating a random-noise signal on a sample-to-sample basis, and then passing the (complex) noise samples through a low-pass digital Butterworth filter with its coefficients selected on the basis of the desired 20-Hz spread.

The sporadic-E signal was modelled as having a single direction, from an apparent 'point source' at 15° elevation, and a Doppler spread of 1.0 Hz. Several different azimuthal separations between the sporadic-E signal and the patch signals were tried: 5, 10 and 15°. Various signal levels were used: 3, 6, 10, 15, 20, and 25 dB below the total spread-source signal.

Background noise was simulated as additive white Gaussian noise which was uncorrelated between antennas. This was set at a level of 40 dB below the total spread-source signal power.

The different simulated signal environments are listed in Table 4.

Table 4: Simulated signal environments

	case 1 15° az. separation	case 2 10° az. separation	case 3 5° az. separation
pt. source: 15° elevation, 0.5-Hz Doppler spread	180° W of N	90° W of N	270° W of N
extended source: 10 - 25° elevation, 20-Hz Doppler spread	140-165° W of N	100-125° W of N	275-300° W of N

6.0 SIMULATION PROCEDURE

The simulation procedure was a two-stage process. The first stage was to model the propagation environment, receiving array, and recording operation, and generate a file consisting of a sequence of simulated signals representing the total signal as seen by the array antennas. The second stage was to operate on the sequence, with the appropriate DF algorithm, in order to obtain a file containing a series of (multiple) direction estimates and other algorithm-related parameters, and to plot that series. The procedure is illustrated in Figures 3 and 4.

6.1 STAGE 1: GENERATION OF RECEIVED SIGNAL DATA

As shown in Figure 3, the information on the array, including the array geometry and the pattern errors, is combined with the assumed patterns (azimuth-independent gain, plane-wave phase response) to derive typical 'actual' patterns. In order to do this, the given rms gain and phase errors are used to derive Fourier coefficients in azimuth space, which define the azimuthal variation in gain and phase away from the assumed pattern, as described previously. The Fourier coefficients, once created, are then stored for later use with the point-source direction or one of the 1000 spread-source directions, to obtain the array response to a signal from that direction.

The defined signal environment provides a discrete direction for the point source, and a range of directions for the spread source; this range is used to generate a randomly placed, uniformly distributed set of 1000 directions. The point source direction and each direction within the spread-source set is used with pattern information to determine the response of each element antenna to that direction.

The defined signal environment provides the relative amplitude and Doppler spreading of the 'point source' signal, and the 'spread source' signal. This information is passed to low-pass-filtered white noise generators, which produce a sequence of signal samples for the point source and for each direction within the spread source, each consistent with a Doppler-spread tone.

The individual array element direction responses, for the point source and for each direction of the spread source, are then combined with the signal samples for each of these directions to obtain the individual signals received by each of the element antennas for each direction. These signals are then added over all the directions, together with the background white-noise samples, to obtain the total signal seen at each antenna.

The resulting signal samples are then stored in a data file for later use with the various direction-finding algorithms.

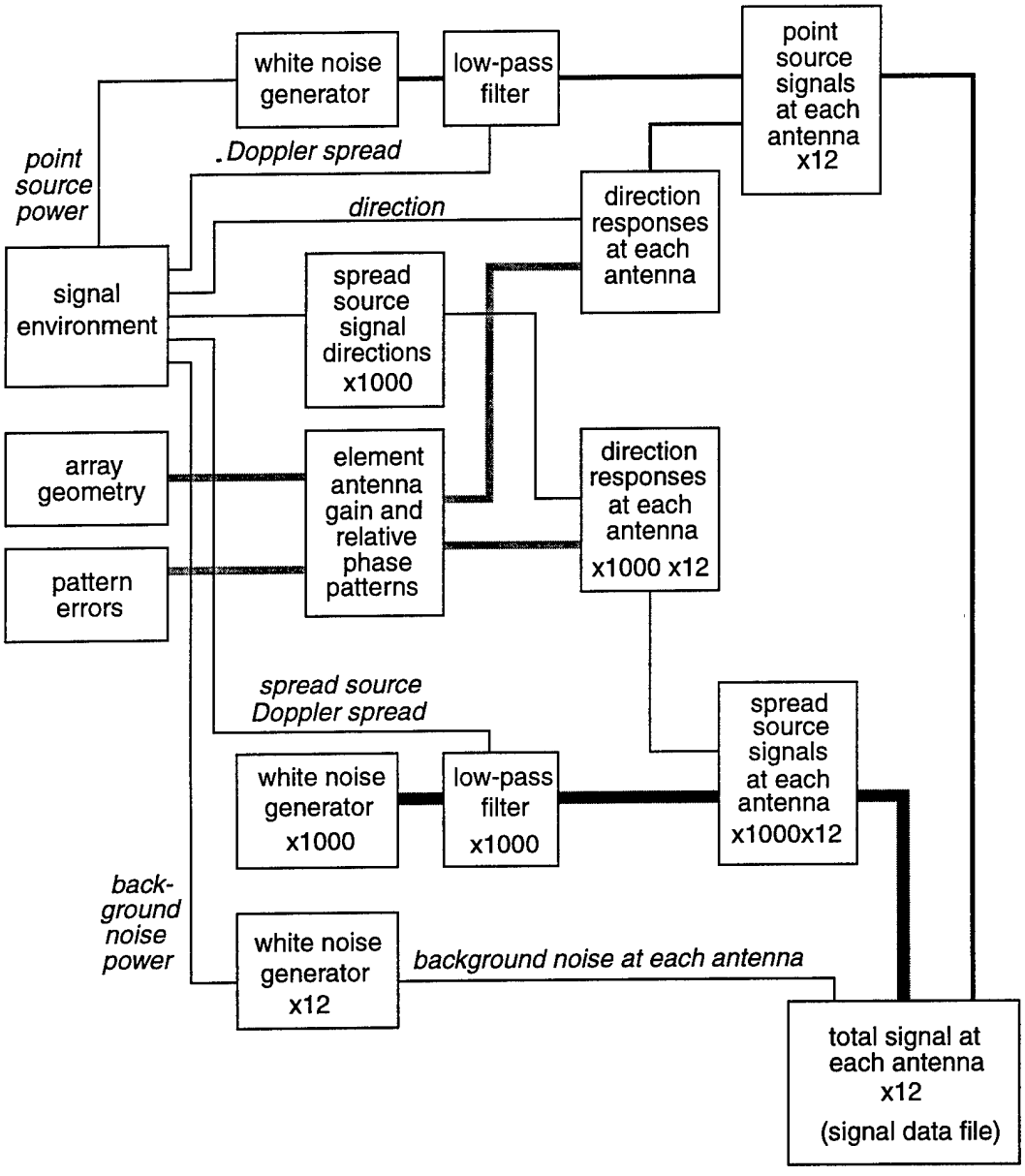

Figure 3. Stage 1 of simulation: signal data generation

The signal data file was given a format identical to that used for previously recorded experimental data, in order to allow the use of DF analysis software originally developed for that data. The sample rate was set at 10k real samples/second per antenna, with the signal being recorded with a center audio frequency of 2.5 kHz. The data was recorded in blocks of 8000 samples x 12 antennas. Normally several blocks of data were recorded with one set of randomly generated antenna patterns (as determined by the Fourier coefficients), then a new set of patterns generated with a new set of Fourier coefficients, and the process repeated. This was done a number of times in each simulation run, so as to prevent the effect of pattern errors being limited to a single set of patterns, and to allow the effects of errors to be viewed in a more statistically significant way. A typical run included 12 blocks (i.e., 9.6 seconds) of data, divided into six 2-block sections each with a different statistically generated set of antenna patterns. This was reduced from the initial 30-block run of six 5-block sections initially used, in order to reduce the computational load in the large number of runs required. (A 30-block run took a single dedicated SPARC 10 workstation approximately 6 hours to complete the generation of its signal data file.)

6.2 STAGE 2: DIRECTION-FINDING OPERATION

The second stage of the simulation, illustrated in Figure 4, was the application of direction-finding techniques to the simulated signal data. The software used for this purpose was developed for use with experimental sampled-aperture data, as well as simulated data [18, 19].

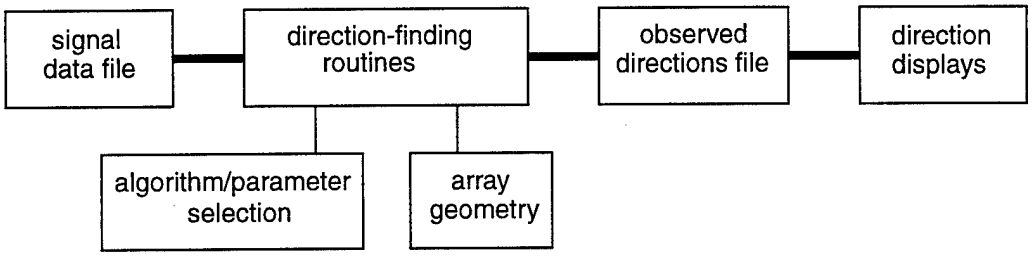

Figure 4. Stage 2 of simulation: direction-finding operation

The direction-finding routines require knowledge of the antenna array geometry and, for this purpose, used the assumed element patterns (azimuth independence of gain, plane-wave phase response). Pattern 'errors' were in this way modelled by the mismatch between these assumed patterns and the 'actual' patterns used to generate the signal data samples.

The direction-finding software contains a number of DF algorithms and a choice of appropriate parameters. The MUSIC algorithm and the maximum-likelihood algorithm were used in the present study. The software first performed a 32-sample Fourier transformation on the incoming signal to select the strongest tone for analysis and increase the signal to noise ratio. Both

algorithms required a covariance matrix to be formed from the resultant tone samples. The algorithms then used the covariance matrix to find the signal directions. Thirty-one tone samples were used in accumulating a covariance matrix, from which a single set of signal directions was estimated. This corresponded to 31 x 32 = 992 signal samples. In order to be consistent with the 8000-sample block size, the next 8 signal samples were ignored before repeating the direction estimation. In this way, the direction-finding operation performed 8 estimates per block, i.e., 10 estimates per second of signal data.

The number of signal directions assumed by the algorithm was estimated using the AIC criterion, as described in Section 4.0, up to a maximum of 8. The number recorded for later display purposes was limited to 6.

7.0 RESULTS

The simulations, as described earlier, were performed for three signal environments each consisting of a number of point-source signal powers relative to the spread source, four array geometries, seven frequencies (or array apertures), and three levels of pattern error. In order to better isolate the effects of these various factors on DF performance, it is helpful to examine the results first in the absence of errors. Once the effects of array geometry and aperture are found, for the different signal environments, the influence of pattern errors can then be considered.

Also, it is important to restrict the analysis to a single DF algorithm, if possible. As will be seen in Section 7.2, the maximum-likelihood algorithm was observed to perform better than the faster MUSIC algorithm, in the modelled signal environments. Being a more optimal approach, maximum likelihood was considered to represent the best that could be achieved, given the assumption of a limited number of directions. It was used for the remainder of the analysis.

7.1 TYPICAL DISPLAYS

The simulation runs were 9.6 seconds in length, with a estimate of directions every 0.1 seconds. Both azimuth and elevation were obtained. Three types of display were developed for interpreting the results; an example of each is given in Figure 5.

For Figure 5, the signal environment consisted of a point source at 180° azimuth and 15° elevation, and a uniformly distributed spread source extending from 140 to 165° in azimuth and 10 to 25° in elevation. The antenna array simulated was the Vortex array (Figure 2) and the DF algorithm used was maximum likelihood.

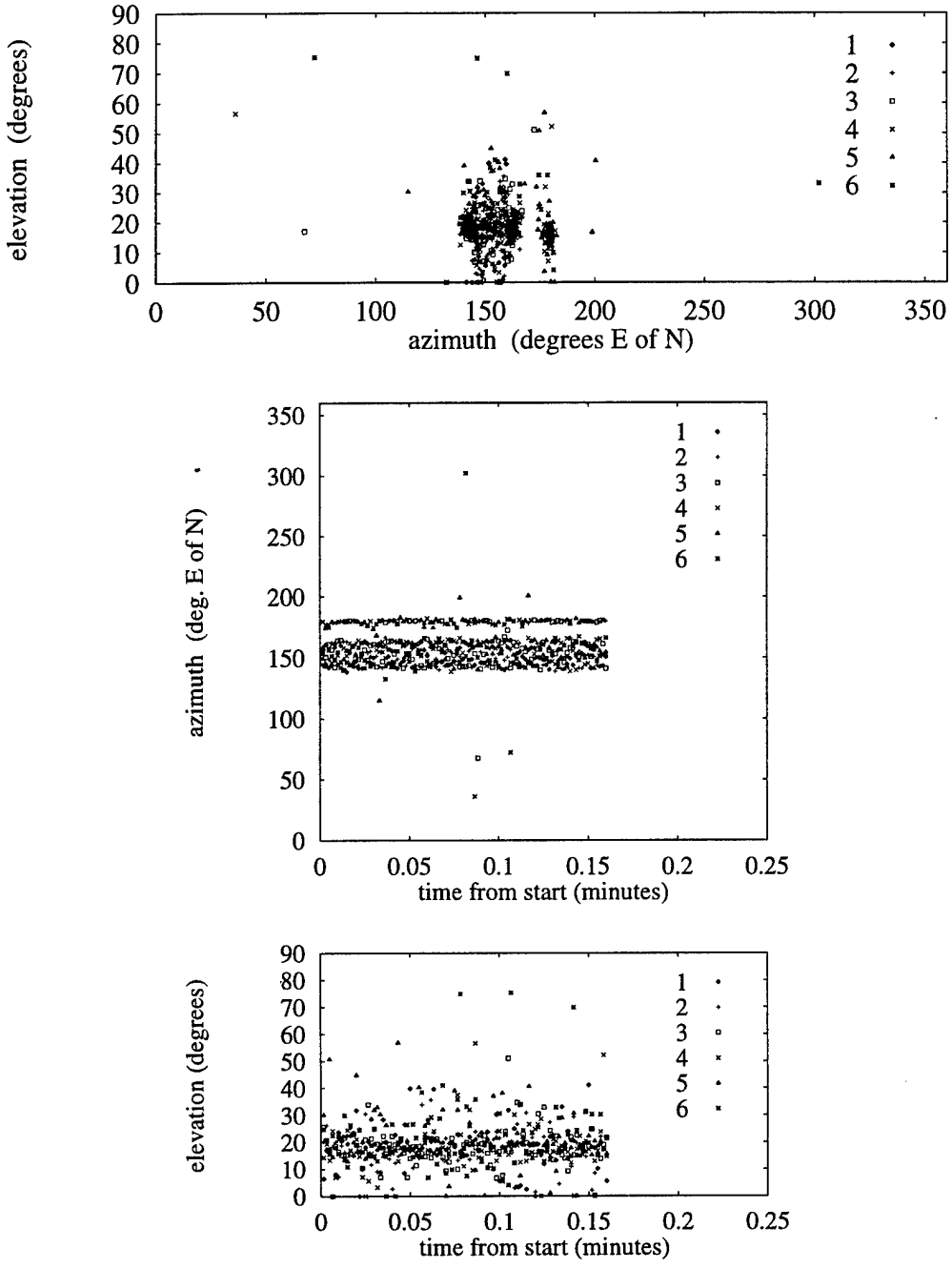

Figure 5. Sample displays of direction results: the Vortex array, 5.0-MHz operating frequency, no pattern errors, receiving a point-source signal from 180° azimuth, 10 dB below a spread-source signal from 140-165° azimuth, using the maximum- likelihood DF algorithm.

The top plot in Figure 5 displays elevation versus azimuth, where the various direction estimates for the run are shown as points. Some of the estimated directions can be seen to cluster about the point-source direction, while many more are seen to cluster about the range of spread-source directions. The middle and bottom plots display the time histories of the azimuth and elevation estimates. The point-source elevation is within the range of spread-source elevations, so the elevation-time plot is not very helpful in distinguishing the point source in the presence of the spread source. However, the point-source azimuth, being 15° outside the spread-source range, is clearly distinct thus allowing the point source to be easily distinguished from the spread source which appears as a roughly uniform distribution of directions over 140 to 165° in azimuth in the Figure 5 azimuth-time plot.

The time histories permit changing conditions to be seen. In the present simulations, they permit the direction estimates from signals simulated with the different sets of statistically generated antenna patterns to be seen separately. For these reasons, the azimuth-time plots were particularly useful in determining performance.

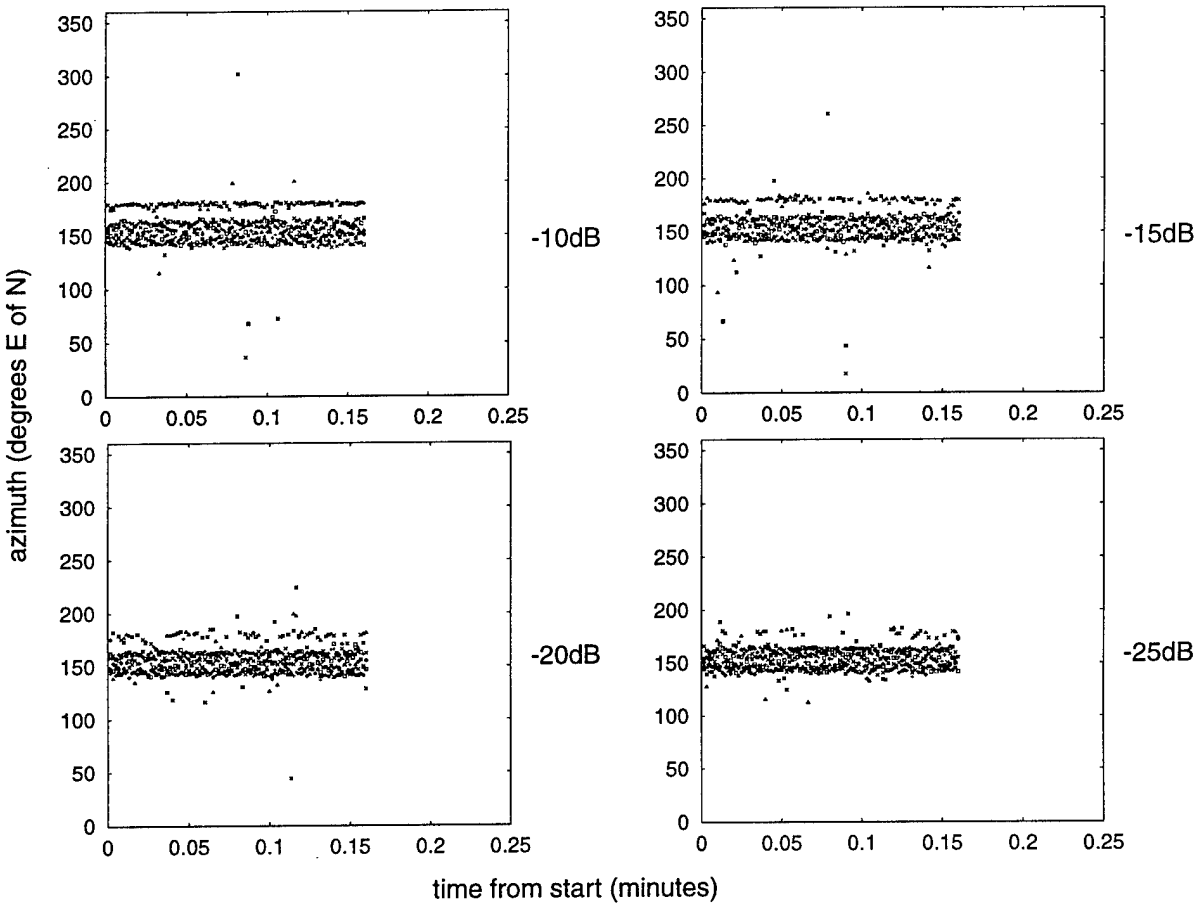

Figure 6. Azimuth-time displays for the Vortex array, 5.0-MHz frequency, no pattern errors. receiving a point-source signal from 180° azimuth and extended-source signals from 140-165° azimuth, for various point-source signal powers relative to the extended source, found using the maximum-likelihood algorithm.

Figure 6 shows several azimuth-time plots, having different point source powers relative to that of the spread source: -10, -15, -20, and -25 dB. When the point source is close in power to the spread source (-10 and -15 dB), it is clearly seen on the azimuth-time display, and its azimuth is clearly defined. As the power is decreased, it becomes less visible, and its azimuth less clearly defined (-20 dB). Eventually it cannot be seen as a point source although a few scattered direction estimates may be attributed to it (-25 dB). From this sequence of azimuth-time plots, the relative power at which it ceases to be visible is determined to be -20 dB.

The relative power of the point source, at which it ceases to be detected as such while in the presence of the stronger spread source, referred to herein as 'point-source visibility', is used as a appropriate measure of performance in the present study. From azimuth-time plots such as those of Figure 6, the point source visibility can be determined within an accuracy of 1 to 2 dB.

7.2 CHOICE OF DF ALGORITHM

Initial studies were made using both the MUSIC and the maximum likelihood algorithms. Since both algorithms make the assumption of a similar number of point-source directions, and the maximum-likelihood approach calculates a more optimal solution, maximum likelihood is expected to yield better performance than MUSIC. The MUSIC algorithm requires much less computation (about 40 times in the cases investigated here) than the very computation-intensive maximum-likelihood approach, which could be sufficient reason for its use provided it does not cause a significant performance deterioration.

Figure 7 contains azimuth-time displays for a situation similar to that of Figure 6 using, in this case, the MUSIC algorithm to determine the signal directions. As can be seen in Figure 7, the MUSIC algorithm is more prone to give rise to false directions, which limits its ability to unambiguously ascertain the presence of weak signals. A false trace at 120° azimuth, equal in its visibility to the point-source trace, is seen in the azimuth time display for a point-source power of -20 dB. Also, when the point source is even weaker, the false trace at 120° is the stronger trace, not very much weaker than the point source trace at -15 dB power. Therefore, the level at which the point source is unambiguously discernable lies, at most, just below - 15 dB. By way of comparison, false direction traces are not evident in the maximum-likelihood estimates illustrated in Figure 6, even at -25 dB point-source power, and the point source remains discernible down to -20 dB.

The case shown here is representative of the other cases compared at other operating frequencies, other array geometries, and with and without pattern errors. The MUSIC algorithm was seen to be much more prone to false directions than maximum likelihood, which limited its ability to unambiguously see weaker signal directions. For this reason, it was decided to restrict the study to the maximum-likelihood technique.

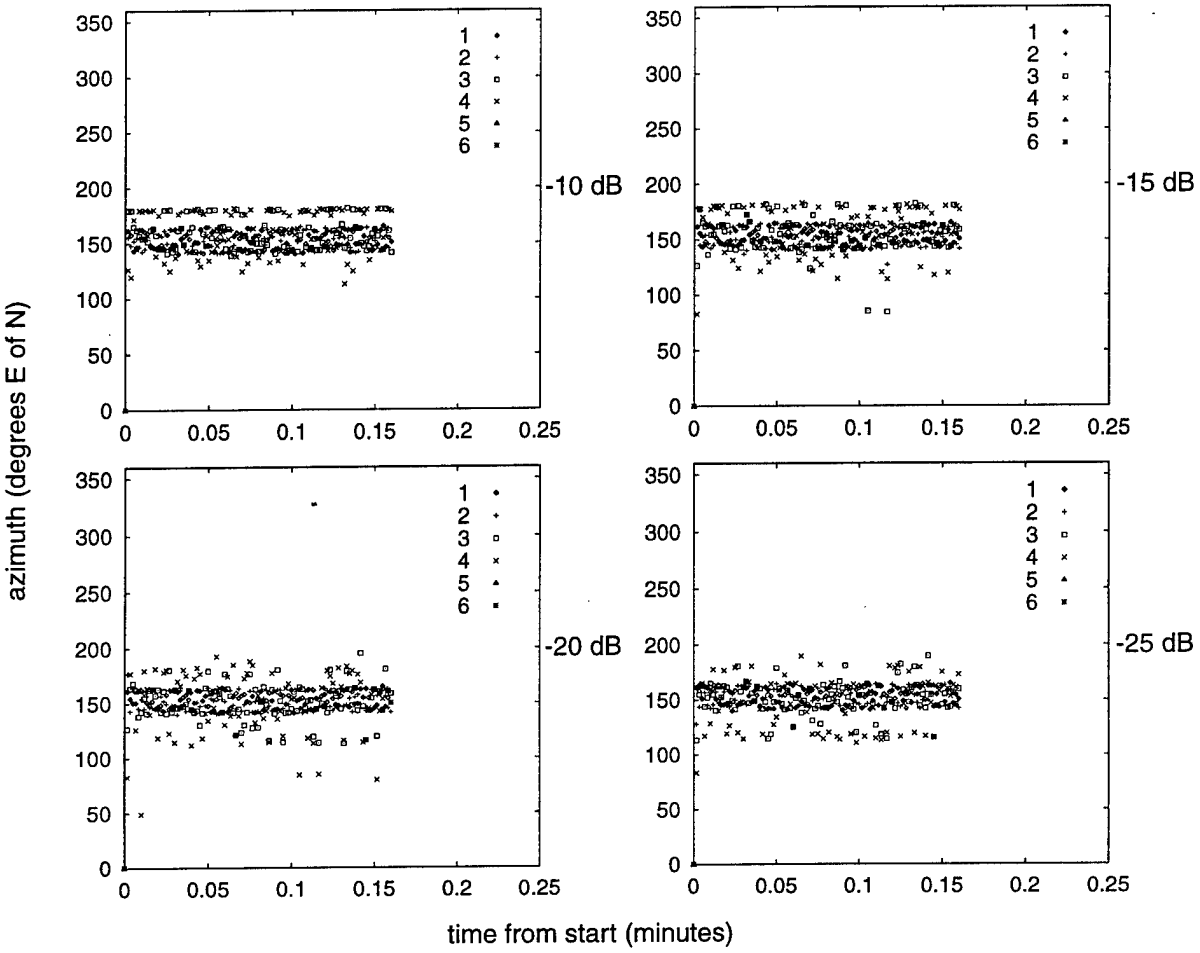

Figure 7. Azimuth-time displays for the Vortex array, 5.0-MHz frequency, no pattern errors, receiving a point-source signal from 180° azimuth and extended-source signals from 140-165° azimuth, for various point-source signal powers relative to the extended source, found using the MUSIC algorithm.

7.3 ERROR-FREE CASE

7.3.1 Effect of Array Aperture

The performance, in terms of the point-source visibility (lowest power relative to the spread source at which the point source could be unambiguously seen) is plotted for the log-spiral array as a function of the array aperture in wavelengths in Figure 8. This figure includes results for the three different signal environments described in Table 4: a 25° -wide spread source and a point separated by 5, 10, or 15° in azimuth from the spread source.

This figure illustrates how the point source visibility depends on the aperture in wavelengths, and on the point-source/spread-source separation. The performance is better when the point source is further removed from the spread source. For each separation, the point-source visibility is relatively poor at the lowest array aperture, and improves as the aperture is increased, up to an optimum value. The optimum value depends on the separation between point source and spread source, being approximately: 2.5 wavelengths for 15° separation, 3.5 wavelengths for 10° separation, and 4.5 wavelengths for 5° separation. As the aperture is increased past the optimum value, the performance deteriorates.

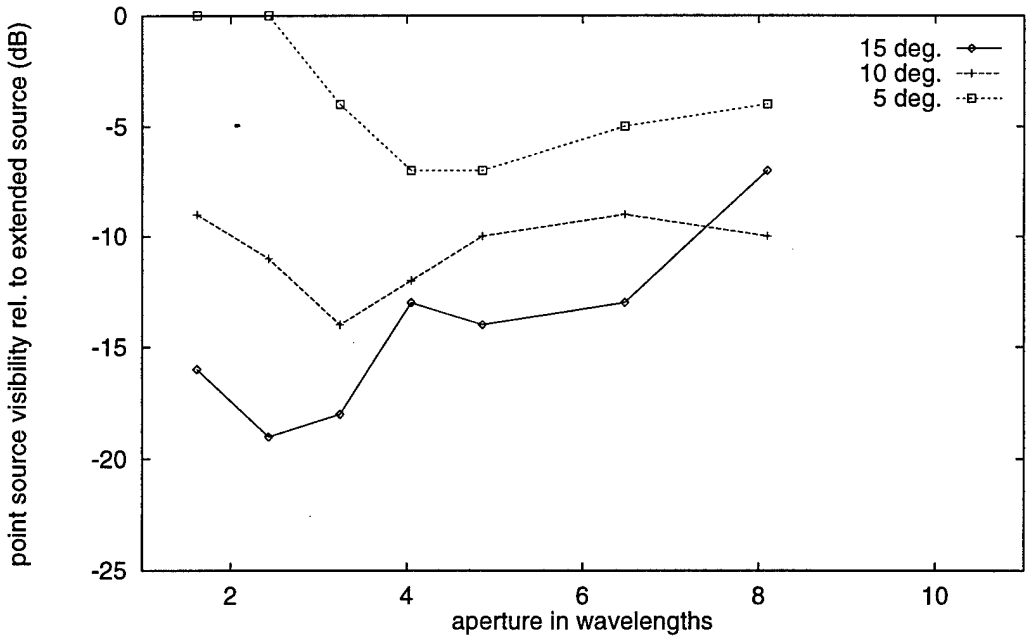

Figure 8. Point-source visibility as a function of array aperture, for the log-spiral array in the presence of a spread source of 25° azimuthal width, and a point source at various separations from the spread source, in the absence of pattern errors.

This behaviour can be explained by two things: the ability of the array to resolve close directions, and the number of directions allocated to the spread source by the DF algorithm. The effects of these features are described in the introduction and are reviewed here, by way of illustration.

When the array aperture in wavelengths is small, the array cannot resolve signals close in direction and, by inference, a weak point source near a spread source. The performance improves as the angular separation of the point-source and spread-source signals is increased. It also improves as the aperture is increased from small values.

The DF algorithm has a limited number of signal directions that it can use to 'describe' the

signal environment. For relatively small array apertures, the effective beamwidth of the array steered to any signal direction is relatively broad, and relatively few steered directions are required to cover a spread-signal source, leaving one or more signal directions available to be used against the weaker point source. When the aperture becomes too large, however, the beamwidth can become so narrow that all the available signal directions are used up in describing the spread source, leaving none for the weaker point source. This explains the reduction in point-source visibility that occurs when the aperture is increased beyond the observed optimum.

The optimum aperture represents a compromise between the conflicting requirements of an aperture sufficient to resolve separated signal directions, and a beamwidth large enough that a spread source can be described by the limited number of directions provided by the present maximum-likelihood DF technique. The optimum aperture increases when the point source is moved closer to the spread source, as a result of the larger aperture required for resolving the two sources in that situation.

7.3.2 Effect of Array Geometry

Figure 9 illustrates the effect of array geometry on DF performance. In this figure, the point-source visibility is plotted as a function of the array aperture in wavelengths, for the four different array geometries tested in this study. Plots are shown for the three modelled point-source/spread-source azimuthal separations.

The general tendencies noted in the previous section for the log-spiral array are observed for the other three arrays as well: an improvement in performance as the aperture is increased from 1.6 wavelengths, to an optimum aperture size which depends on the point-source/spread-source separation, and then a subsequent deterioration in performance as the aperture is increased past the optimum.

The two experimental arrays (Vortex and log-spiral) each have their closest spacings in the center of the array (see Figure 2). They tend to be similar in their ability to see a weak point source in the presence of a spread source, at a point-source/spread-source azimuthal separation of 15°. The Vortex array is worse than the log-spiral array (and other arrays) for smaller azimuthal separations, which may be related to the large number of close spacings for this array.

The circle array does not have the small spacings that the other arrays have. Its performance is relatively better than the experimental arrays when the aperture is small. However, it quickly becomes the same as, or worse than, the experimental arrays in seeing the point source when the aperture is increased.

The three-pronged star array, unlike the other experimental arrays, has more closely-spaced elements at its outer edges (Figure 2), which results in a greater number of large inter-element spacings for this array. It performs similarly, or better than the other arrays at small apertures, and becomes much better than the other arrays at seeing a weak point source when the aperture is increased.

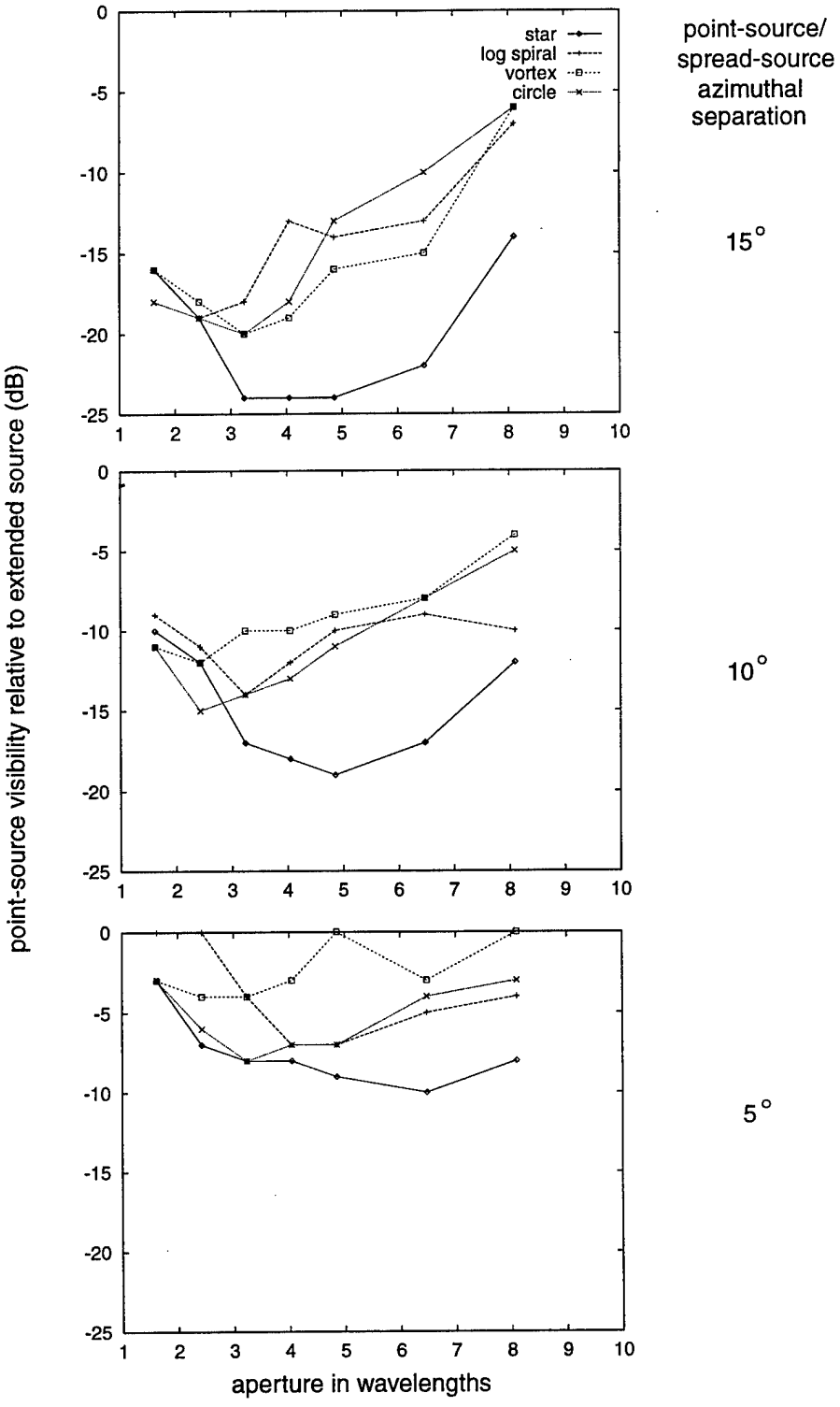

Figure 9. Point-source visibility as a function of array aperture, for the various array geometries in the absence of pattern errors.

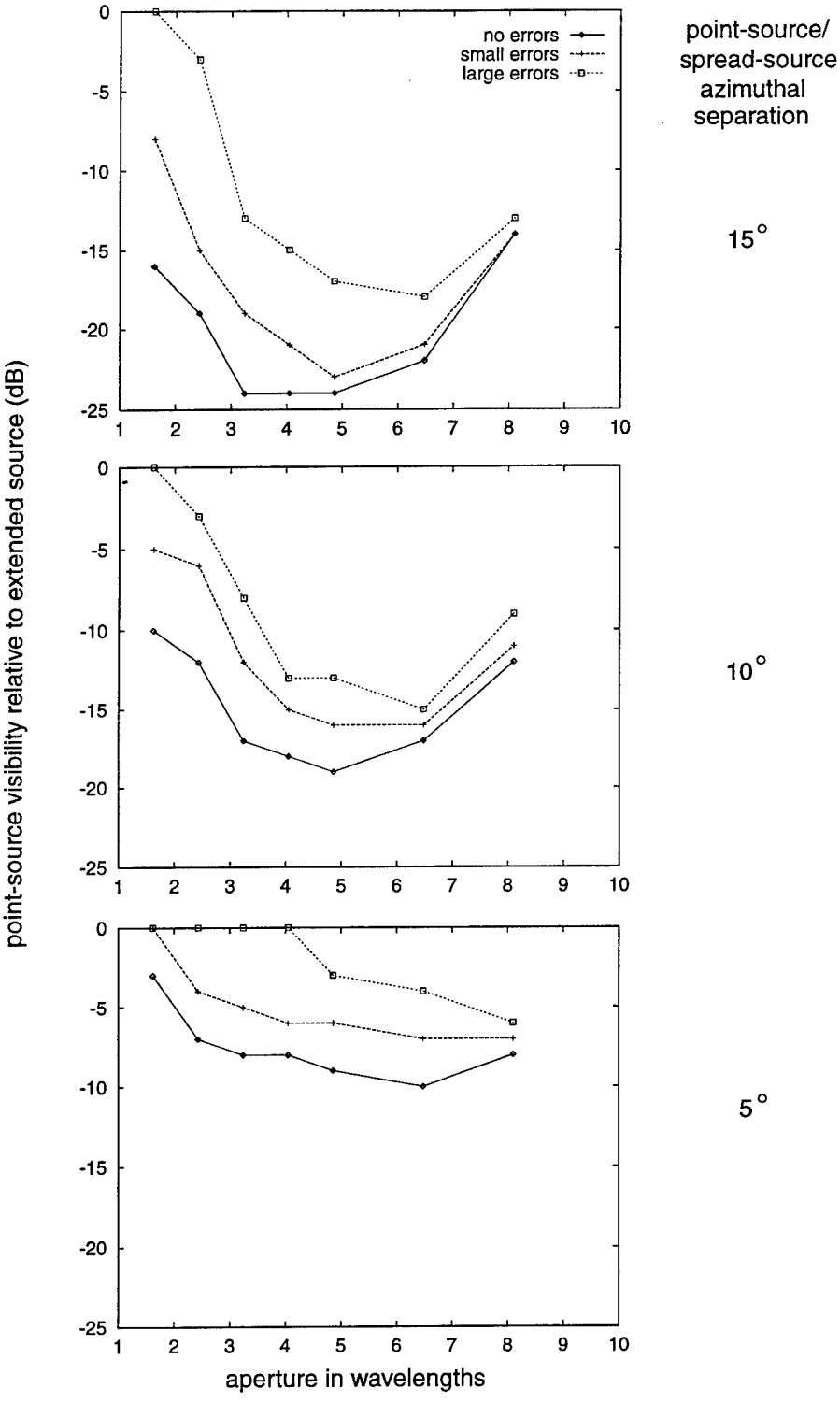

Figure 10a. Point-source visibility as a function of array aperture, for the star array with various levels of pattern error.

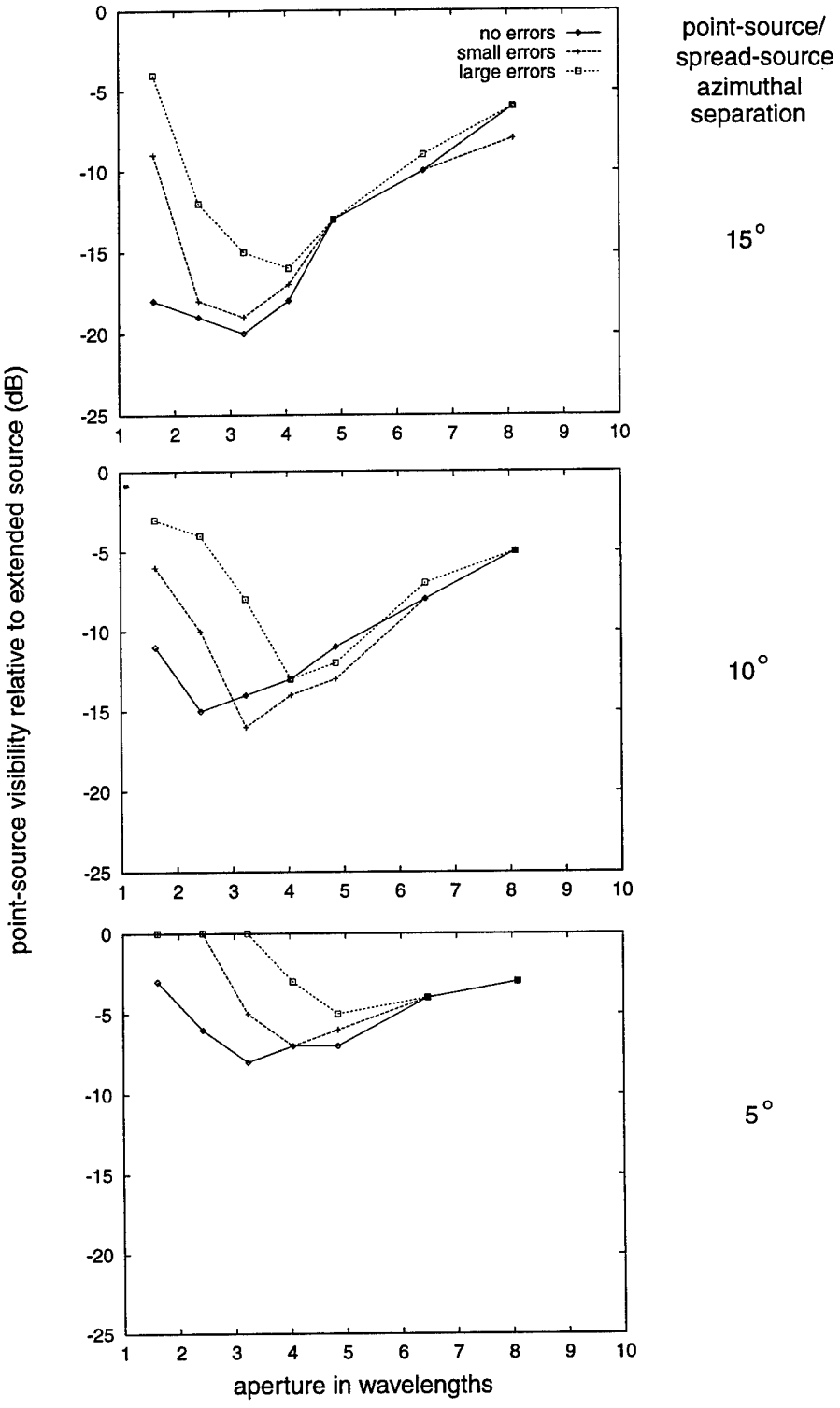

Figure 10b. Point-source visibility as a function of array aperture, for the circle array with various levels of pattern error.

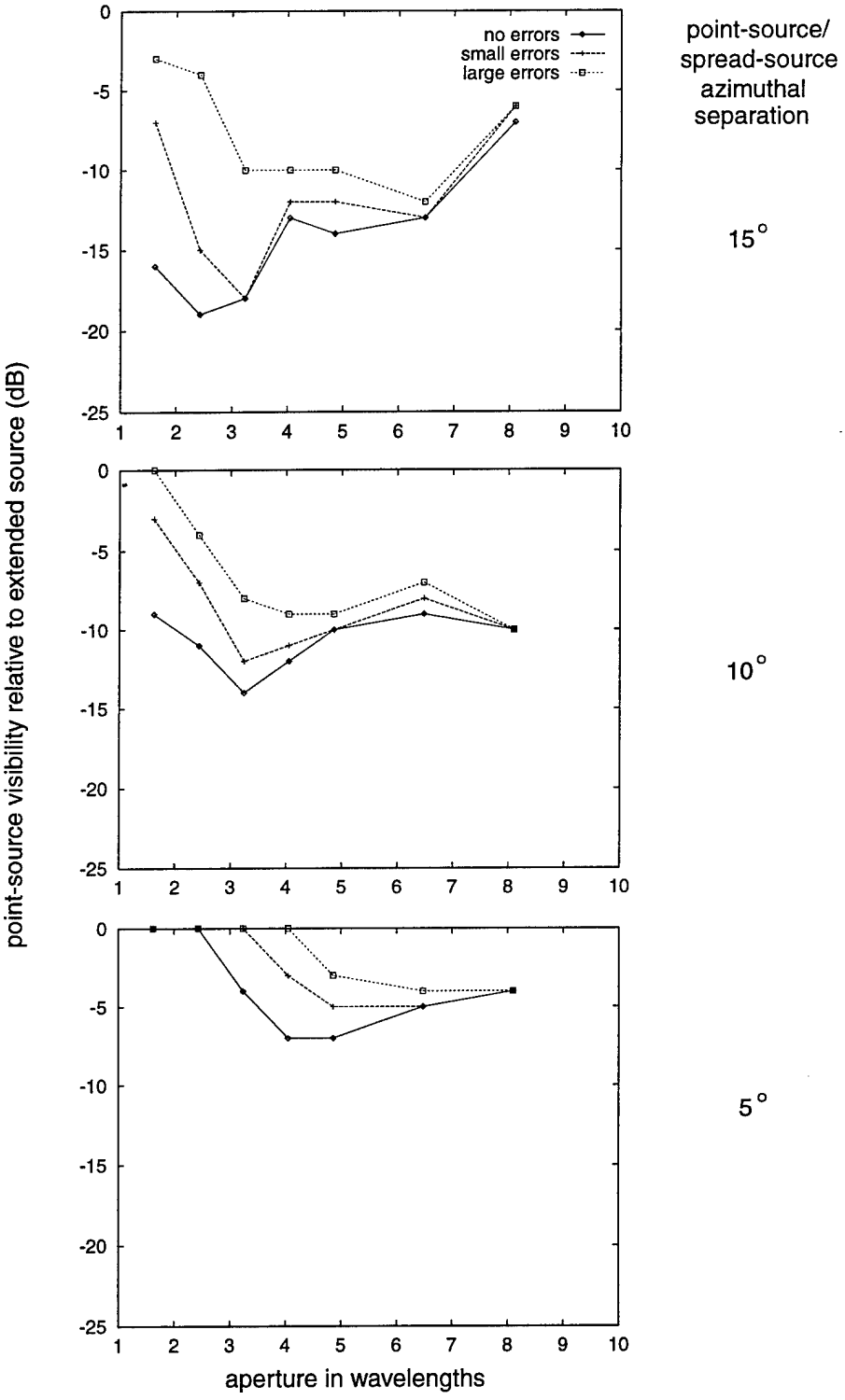

Figure 10c. Point-source visibility as a function of array aperture, for the log-spiral array with various levels of pattern error.

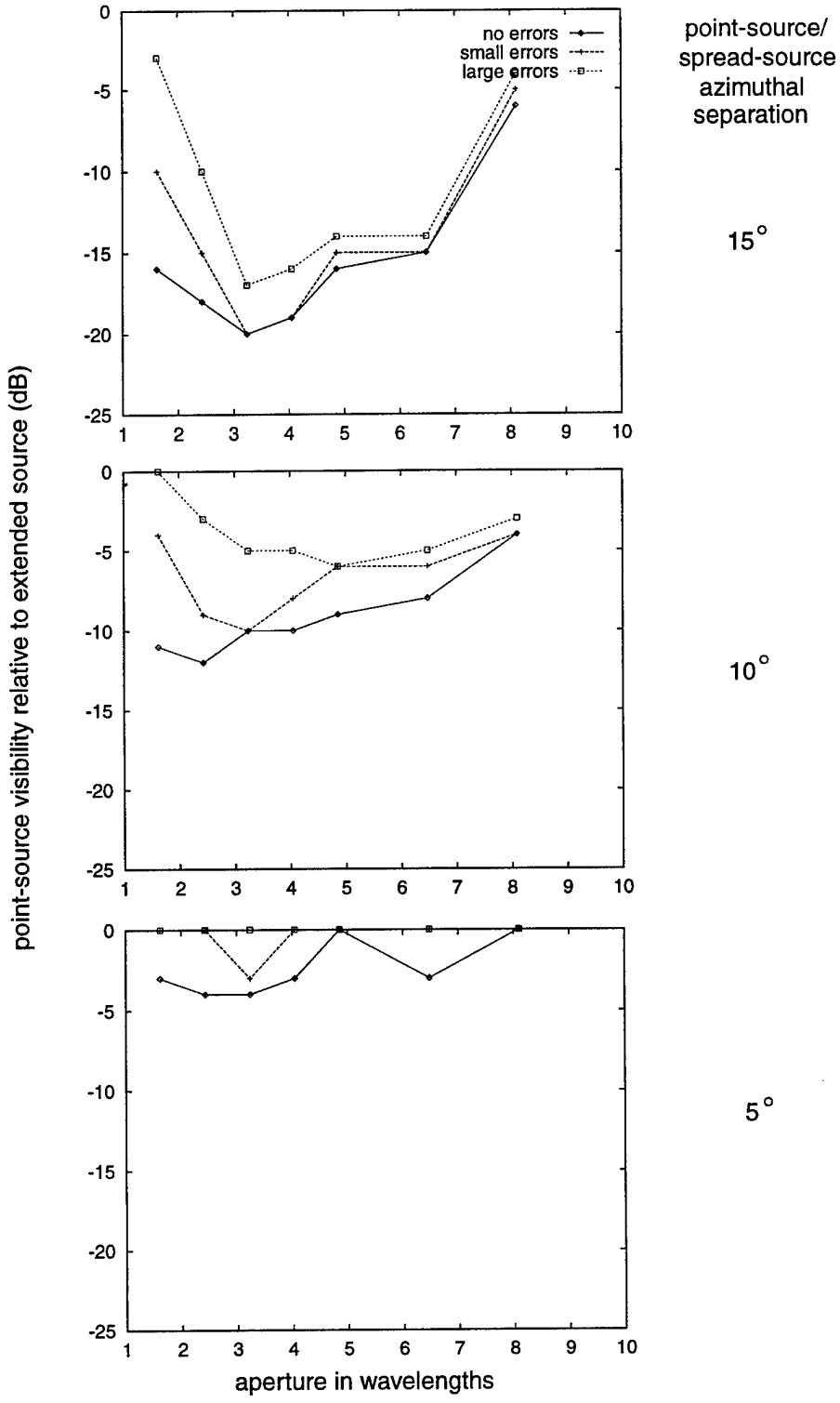

Figure 10d. Point-source visibility as a function of array aperture, for the Vortex array with various levels of pattern error.

7.4 INFLUENCE OF PATTERN UNCERTAINTIES

Figures 10a, b, c and d show the effect of element antenna pattern uncertainties, or errors, on DF performance for the four array geometries tested. These figures contain curves of point source visibility versus array aperture in wavelengths for the situations of no pattern errors, small pattern errors, and large pattern errors, the values of which are listed in Section 2.0, Table 3. Plots are shown for each of the three point-source/spread-source azimuthal separations: 15°, 10°, and 5°.

Figure 10a, for the star array, is illustrative of the influence of antenna pattern uncertainties on performance. Pattern uncertainties are noted to reduce the point-source visibility: the point source is not seen in the presence of the stronger extended source at as low a power when antenna pattern errors exist that it is when there are no pattern errors. The deterioration in performance is greatest when the array aperture in wavelengths is small. At apertures less than 3 wavelengths, the point-source visibility is reduced by 10 dB or more by large pattern errors. As the array aperture increases past 5 wavelengths, the effect of the simulated pattern errors on performance becomes quite small, with the performance reduction due to large pattern errors dropping from 5 to 2 dB. The curves for the three signal separations, although very different, show a roughly similar deterioration in performance due to pattern errors.

In the previous section, the star array was noted to have the best performance of the four arrays in the absence of errors. In comparing Figure 10a, showing the effect of errors on performance for the star array, with Figures 10b, c and d, for the circle, log-spiral, and Vortex arrays respectively, it is clear that these three arrays do not suffer as great a reduction in performance when pattern errors are added as does the star array. This is especially true at the medium to large apertures where the star array outperforms the other arrays in the absence of errors. The effect of pattern errors on performance is even more strongly dependent on aperture for these three arrays, with a typical performance reduction, due to large errors, of approximately 10 dB at apertures of less than 3 wavelengths and 1 dB or less at apertures of 5 or more wavelengths.

The lack of a noticeable effect of pattern errors on DF performance at larger array apertures is most marked for the circle array, illustrated in Figure 10b. This is likely related to the fact that this array, unlike the others, contains no very closely spaced elements. (Closely spaced elements are more prone to error effects, since a relative phase error or an amplitude error between two closely spaced elements can be shown to translate into a greater direction error than if the elements were further apart.)

The greater effect of errors on the star array's performance raises the issue as to whether the star array still performs better than the other arrays in the presence of errors. This is considered in Figures 11 and 12, which show the point-source visibility as a function of array aperture for the four array geometries in the presence of small and large errors respectively. These figures may be compared with Figure 9 which illustrates the case of no pattern errors.

In Figure 9, the star array is seen to perform considerably better than the other arrays in the absence of errors, particularly at medium to large apertures. In Figure 11, where small pattern

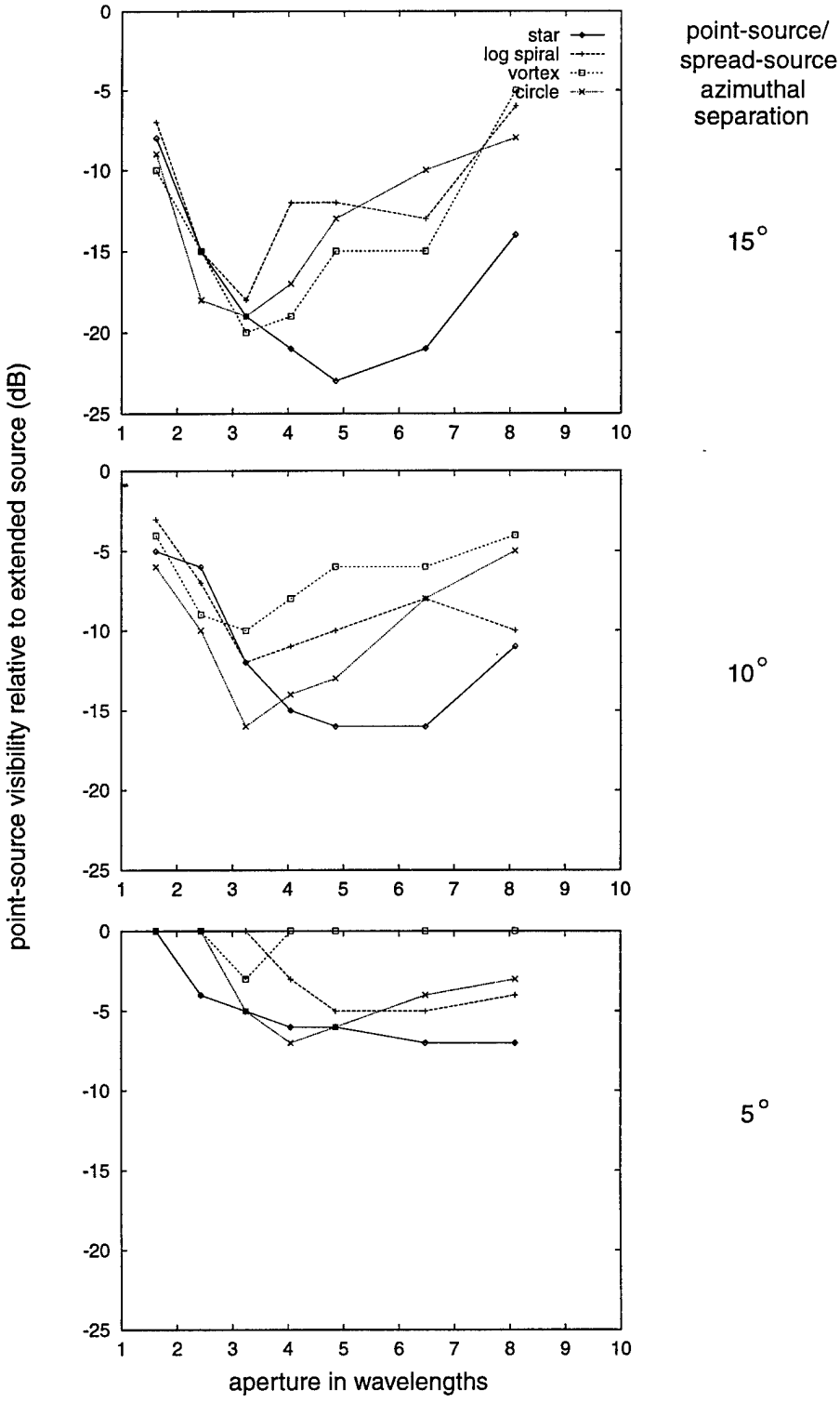

Figure 11. Point-source visibility as a function of array aperture, for the various array geometries with small pattern errors.

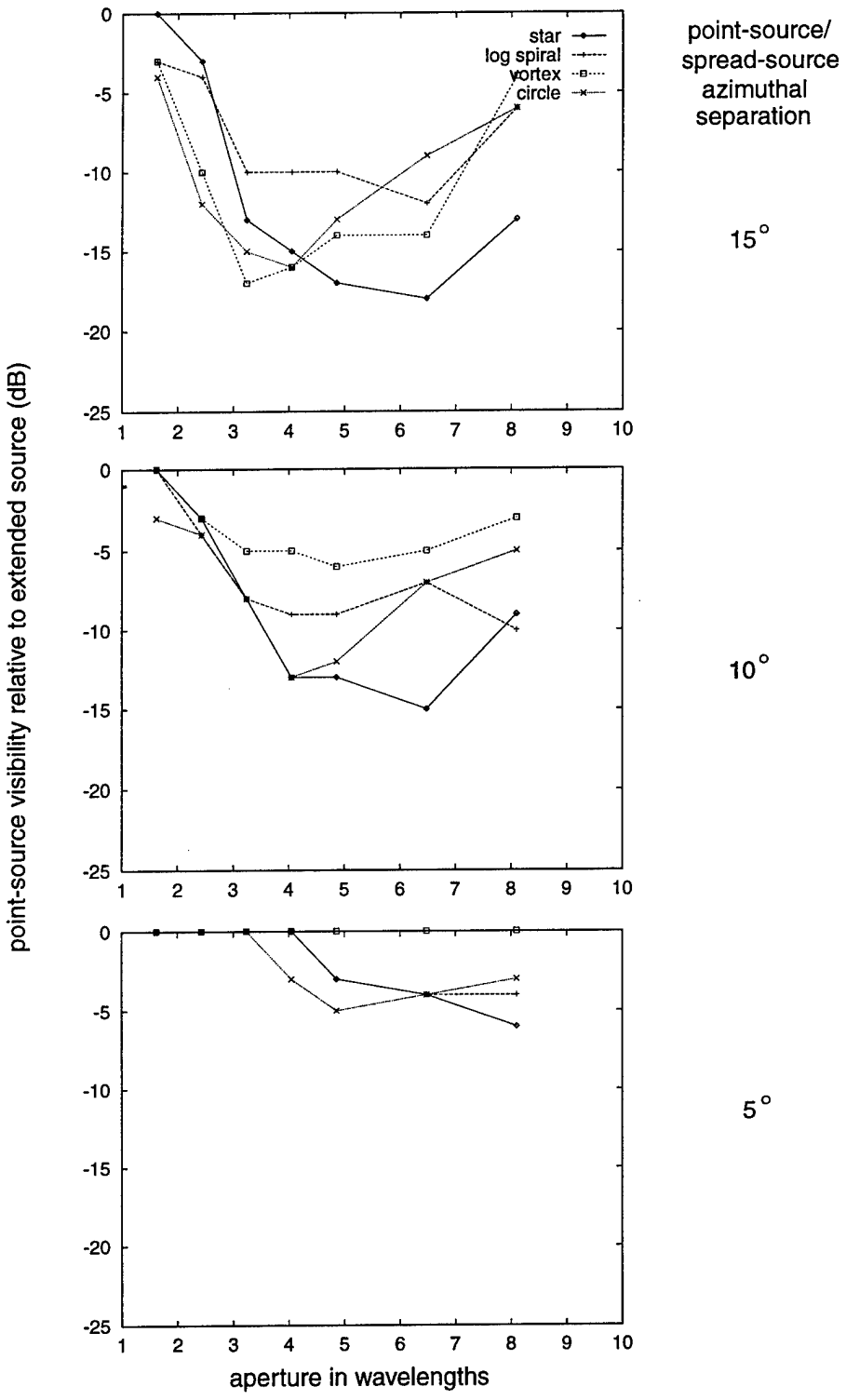

Figure 12. Point-source visibility as a function of array aperture, for the various array geometries with large pattern errors.

errors are included, the star array's performance is seen to continue to be better than that of the other arrays, although not as much as in the absence of errors. In Figure 12, where large pattern errors are included, the star array's performance at medium to large apertures remains better than that of the other arrays, at least for the 15 and 10° point-source/spread-source separations.

From Figure 9 it is evident that the star array has a much better performance than the other arrays in the absence of errors, so that it has 'more to lose' when errors are added. This is clearly the case as is seen in Figures 10a through d. However, even with pattern errors, it continues to perform better than the other arrays, as is seen in Figures 11 and 12.

As the effect of pattern errors is less for larger array apertures, it is important to choose an array geometry that performs well with a large aperture. The star array, more than the other geometries, meets this requirement.

8.0 DISCUSSION

The present simulation study has concerned itself with developing appropriate array geometries for improving DF performance in the difficult propagation conditions presented by the nighttime high-latitude ionosphere. Spread sources, consisting of multiple signal directions reflected or scattered from moving ionospheric blobs or patches, are present and yield unreliable transmitter bearings. Weaker signals propagating via sporadic-E reflections may be present at these times, and yield accurate transmitter bearings. The requirement on the DF array and estimation algorithm is to detect and identify the sporadic-E signal direction in the presence of the stronger spread-source signal directions.

This study has demonstrated that array aperture and geometry are critical factors in the ability of an array to identify such directions. The performance is limited on the small-aperture side by the resolving power of the array, and limited on the large-aperture side by the resulting narrow array beamwidth requiring all available signal directions (less than the number of antennas) to be used up in attempting to cover a stronger spread source of signal directions, thereby leaving none for a weaker (sporadic E) point source. The array geometry was observed also to influence point-source visibility; the best performance in terms of point-source visibility was noted for the three-pronged star geometry of Figure 2. As well as having the best performance in its useful range of apertures, this geometry was noted to have the largest range of apertures over which good performance was achieved.

The effect of pattern uncertainties was observed to have a significant effect on point-source visibility, being quite pronounced at small apertures, and less so at larger apertures. Pattern uncertainties applied to the simulation were similar to those deduced from measurement of the Vortex array, which had a large number of closely spaced elements with strong interactions. The pattern uncertainties of a potential operational array may be reduced if a configuration is selected which does not have the close element spacings of the Vortex array, and if the array aperture can be increased (which increases the element spacings). The star array is a good choice for both these reasons.

Areas of further study include the development and investigation of multiple-direction DF algorithms based on spread sets of directions rather than single directions. Initial work based on an approach developed at DREO [18] has already been carried out, and simulation work similar to the present study is under way for these algorithms. Another area of investigation is the examination of high-latitude nighttime records to determine the incidence of sporadic-E. This may be done using oblique ionogram data as well as the limited amount of sampled-aperture DF data available.

REFERENCES

[1] Tsunoda, R. T., *High Latitude F Region Irregularities: A Review and Synthesis*, Rev. Geophys., Vol. 26, No. 4, pp. 719-760, 1987.

[2] Kelly, M. C., *The Earth's Ionosphere: Plasma Physics and Electrodynamics*, Academic Press, 1989.

[3] Jenkins, R. W., *A Simulation Study of HF Direction-Finding in the Presence of F-Region Scattering and Sporadic-E*, CRC Report 93-004, 1994.

[4] Gething, P.J., *Radio Direction Finding and Superresolution*, IEE Electromagnetic Wave Series 33, 2nd. ed. Peter Peregrinus Ltd., 1991.

[5] Jenkins, R.W., *Antenna Amplitude and Phase Pattern Measurements Using an Aircraft-Towed Transmitter*, CRC Report 95-003, 1995.

[6] Jenkins, R.W., and L.E. Petrie, *A Comparison of Modelled and Measured HF Antenna Array Patterns*, CRC Technical Note 96-002, 1996.

[7] Jenkins, R.W., and L.E. Petrie, *Measurement and Modelling of HF Antenna Gain and Phase Patterns and the Effect on Array Performance*, Proc. IEE Conf. Antennas and Propagation, IEE Conf. Publication No. 436, pp 1.409-1.411, 1997.

[8] Heppner, J.P., and N.C. Maynard, *Empirical High-Latitude Electric Field Models*, J. Geophys. Res., Vol. 32, No. A5, pp. 4467-4489, 1987.

[9] Rodger, A.S., et al., *A New Mechanism for Polar Patch Formation*, J. Geophys. Res., Vol. 99, No. A4, pp. 6425-6436, 1994

[10] Muldrew, D.B., and J.F. Vickrey, *High-Latitude F Region Irregularities Observed Simultaneously with ISIS 1 and the Chatanika Radar*, J. Geophys. Res., Vol. 87, No. A10, pp. 8262-8272, 1982.

[11] Wu, Q., et al., *Intensification and Fading of Auroral Arcs in the Dusk-Midnight Sector of the Polar Cap*, J. Geophys. Res., Vol. 96, No. A5, pp. 7709-7717, 1991.

[12] Jenkins, R.W., *Preliminary Analysis of Kestrel Data*, informal CRC Technical Memorandum DRL/TM083/92, 1992.

[13] Read, W., personal communication, Defence Research Establishment Ottawa, 1997.

[14] Schmidt, R.O., *Multiple Emitter Location and Signal Parameter Estimation*, IEEE Trans. Antennas and Propagation, Vol. AP-34, pp. 276-280, 1986.

[15] Ziskind, I., and M. Watt, *Maximum Likelihood Localization of Multiple Sources by Alternating Projection*, IEEE Trans. Acoustics Speech and Signal Processing, Vol. ASSP-36, pp. 1553-1560, 1988.

[16] Akaike, H., *Information Theory and an Extension of the Maximum Likelihood Principle*, Proc. 2nd Int. Symp. Inform. Theory, suppl. Problems of Control and Inform. Theory, pp. 267-281, 1973.

[17] Lawley, D.N., *Tests of Significance of the Latent Roots of the Covariance and Correlation Matrices*, Biometrica, Vol. 43, pp. 128-136, 1956.

[18] Dumas, D., *High-Latitude HF Direction-Finding: A Case Study and Modelling Results*, Proc. 2nd Symp. Radiolocation and Direction Finding, SWRI, San Antonio, Tx., Session 1, Paper 2, 1997.

[19] Dumas, D., CRC Report under preparation, 1997

UNCLASSIFIED

SECURITY CLASSIFICATION OF FORM
(highest classification of Title, Abstract, Keywords)

DOCUMENT CONTROL DATA

(Security classification of title, body of abstract and indexing annotation must be entered when the overall document is classified)

1. ORIGINATOR (the name and address of the organization preparing the document. Organizations for whom the document was prepared, e.g. Establishment sponsoring a contractor's report, or tasking agency, are entered in Section 8)

COMMUNICATIONS RESEARCH CENTRE
3701 CARLING AVENUE
P.O. BOX 11490, STATION H
OTTAWA, ONTARIO
CANADA K2H 8S2

2. SECURITY CLASSIFICATION (overall security classification of the document including special terms if applicable)

UNCLASSIFIED - UNLIMITED DISTRIBUTION

3. TITLE (the complete document title as indicated on the title page. Its classification should be indicated by the appropriate abbreviation (S,C,R or U) in parentheses after the title)

THE EFFECTS OF ANTENNA ARRAY GEOMETRY AND ELEMENT PATTERN UNCERTAINTY ON HIGH-LATITUDE HF DIRECTION FINDING (U)

4. AUTHORS (Last name, first name, Middle initial)

ROBERT W. JENKINS

5. DATE OF PUBLICATION (month and year of publication of document)

DECEMBER 1997

6a. NO. OF PAGES (total containing information. Include Annexes, Appendices, etc.)

29

6b. NO. OF REFS. (total cited in document)

19

7. DESCRIPTIVE NOTES (the category of the document, e.g. technical report, technical note or memorandum. If appropriate, enter the type of report, e.g. interim, progress, summary, annual or final. Give the inclusive dates when a specific reporting period is covered.)

CRC-RP-97-006

8. SPONSORING ACTIVITY (the name of the department project office or laboratory sponsoring the research and development. Include the address.)

DEFENCE RESEARCH ESTABLISHMENT OTTAWA(DREO)
3701 CARLING AVENUE
OTTAWA, ONTARIO
K1A 0Z4

9a. PROJECT OR GRANT NO. (if appropriate, the applicable research and development project or grant number under which the document was written. Please specify whether project or grant)

661-990-X77-998445419 - WK UNIT #5bd14

9b. CONTRACT NO. (if appropriate, the applicable number under which the document was written)

10a. ORIGINATOR'S DOCUMENT NUMBER (the official document number by which the document is identified by the originating activity. This number must be unique to this document) CRC REPORT 97-006

10b. OTHER DOCUMENT NOS. (Any other numbers which may be assigned to this document either by the originator or the sponsor)

11. DOCUMENT AVAILABILITY (any limitations on further dissemination of the document, other than those imposed by security classification)

(X) Unlimited distribution
( ) Distribution limited to defence departments and defence contractors; further distribution only as approved
( ) Distribution limited to defence departments and Canadian defence contractors; further distribution only as approved
( ) Distribution limited to government departments and agencies; further distribution only as approved
( ) Distribution limited to defence departments; further distribution only as approved
( ) Other (please specify)

12. DOCUMENT ANNOUNCEMENT (any limitation to the bibliographic announcement of this document. This will normally correspond to the Document Availability (11). However, where further distribution (beyond the audience specified in 11) is possible, a wider announcement audience may be selected.)

UNLIMITED

UNCLASSIFIED

SECURITY CLASSIFICATION OF FORM

DCD03 2/06/87

UNCLASSIFIED
SECURITY CLASSIFICATION OF FORM
(highest classification of Title, Abstract, Keywords)

13. ABSTRACT (a brief and factual summary of the document. It may also appear elsewhere in the body of the document itself. It is highly desirable that the abstract of classified documents be unclassified. Each paragraph of the abstract shall begin with an indication of the security classification of the information in the paragraph (unless the document itself is unclassified) represented as (S), (C), (R), or (U). It is not necessary to include here abstracts in both official languages unless the text is bilingual).

Simulation studies are described which model the performance of a sampled-aperture HF direction-finding (DF) system operating with specified array geometries in the presence of both single-reflection (point source) and multiple reflection/scattering (extended source) ionospheric radio propagation typical of observed high-latitude night-time conditions. A multiple-direction estimator was used to obtain direction estimates; the deterministic maximum likelihood algorithm was selected for this, following a comparison between it and the MUSIC algorithm. Array pattern errors, based on previous phase and amplitude pattern measurements and numerical modelling, were included in the simulation. The performance is characterised in terms of the ability of the DF system to see a weaker point source in the presence of the extended source. The array apertures in wavelengths (or alternately operating frequencies for a fixed-size array) over which good performance was obtained was limited at the low end by the resolving power of the array, and at the high end, by the narrow array beamwidth and the limited number of directions available to the DF algorithm to describe the situation. pattern errors reduced performance significantly; much more at small array apertures (2.5 wavelengths or less) than at larger apertures (5 wavelengths or more). Of the four 12-element array geometries tested, the 'star' array, consisting of three arms with its smallest spacings at its extremities, performed best over the widest range of aperture sizes (or alternately, operating frequencies).

14. KEYWORDS, DESCRIPTORS or IDENTIFIERS (technically meaningful terms or short phrases that characterize a document and could be helpful in cataloguing the document. They should be selected so that no security classification is required. Identifiers, such as equipment model designation, trade name, military project code name, geographic location may also be included. If possible keywords should be selected from a published thesaurus, e.g. Thesaurus of Scientific Terms (TEST) and that thesaurus-identified. If it is not possible to select indexing terms which are Unclassified, the classification of each should be indicated as with the title.)

HF Radio
HF Direction-Finding
High Latitude HF Radio Propagation
HF Antenna Patterns
HF Antenna Arrays
Antenna Pattern Errors